



HAL
open science

Modified upright cup method for testing water vapor permeability in porous membranes

Zoughaib Assaad, Rasha Mustapha, Assaad Zoughaib, Nesreen Ghaddar,
Kamel Ghali

► **To cite this version:**

Zoughaib Assaad, Rasha Mustapha, Assaad Zoughaib, Nesreen Ghaddar, Kamel Ghali. Modified upright cup method for testing water vapor permeability in porous membranes. *Energy*, 2020, 195, pp.117057. 10.1016/j.energy.2020.117057 . hal-02470739

HAL Id: hal-02470739

<https://hal.science/hal-02470739>

Submitted on 7 Mar 2022

HAL is a multi-disciplinary open access archive for the deposit and dissemination of scientific research documents, whether they are published or not. The documents may come from teaching and research institutions in France or abroad, or from public or private research centers.

L'archive ouverte pluridisciplinaire **HAL**, est destinée au dépôt et à la diffusion de documents scientifiques de niveau recherche, publiés ou non, émanant des établissements d'enseignement et de recherche français ou étrangers, des laboratoires publics ou privés.



Distributed under a Creative Commons Attribution - NonCommercial 4.0 International License

Modified Upright Cup Method for Testing Water Vapor Permeability in Porous Membranes

Rasha Mustapha^{1*}, Assaad Zoughaib¹, Nesreen Ghaddar², Kamel Ghali²

⁽¹⁾ MINES ParisTech-PSL Research University-CES, Palaiseau, France,

rasha.mustapha@mines-paristech.fr,

assaad.zoughaib@mines-paristech.fr

⁽²⁾ Faculty of Engineering and Architecture, American University of Beirut, Beirut, Lebanon,

farah@aub.edu.lb

ka04@aub.edu.lb

Abstract

A membrane based heat and mass exchanger is a promising technology used to control both sensible and latent loads. Membranes are porous materials that allow water vapor transmission from one medium to another. Water vapor permeability of these membranes is the key parameter for establishing their performance. Various techniques exist to measure the water vapor permeability in membranes of different types and characteristics. The most commonly used is the cup test based on the standards published by The American Society for Testing and Materials (ASTM). The upright cup test described in the ASTM E96 standard is mainly used to predict the values of low to moderate permeable materials where the air resistance above the cup is relatively small. This paper briefly describes the ASTM test and introduces a modified technique that infers the water vapor transmission in highly permeable materials considering explicitly the air resistance. Different porous materials, initially manufactured for considerations other than operating as membranes, are identified and experiments are conducted to derive their permeability using an identification method. The results of the experiments are subjected to an uncertainty analysis to assess the accuracy of the measuring technique showing acceptable values ranging from 8% to 26%.

Keywords: Water vapor permeability; Water vapor transmission rate; Cup method; Membrane; ASTM E96.

1. Introduction

The global energy consumption has risen significantly in the past decades due to the growth of population, to the increase in the thermal comfort desire and to the rapidly developing economy. Buildings account for 20 to 40% of the total energy consumption and the time spent indoors is increasing [1]. Thus the energy consumed by residential and non-residential buildings is expected to increase by 67% and 33% in 2030 [2], [3]. The heating, ventilation and air conditioning (HVAC) systems are responsible for around 50% of the energy consumed in buildings and conventional vapor compression cycles are the most commonly used systems [4]. Yet, these

systems can efficiently handle the sensible load but when it comes to indoor humidity control they show some deficiencies [5]. In order to extract humidity, vapor compression cycles lower the air temperature below its dew point temperature to remove its moisture by the condensation process and then reheat it to reach the desired indoor comfort temperature [6]. This process consumes around 20 to 40% of the total energy and increases peak electricity demands [7]. Consequently, to lower the energy consumed in buildings it is essential to reduce the energy consumption of the HVAC system [8]. Thus providing healthy indoor environment with low energy demand is a considerable engineering challenge. Hybrid air conditioning systems (liquid desiccant and vapor compression cycle) using porous membrane based heat and mass exchangers may be ideal alternatives to traditional air conditioning systems decreasing the energy consumption [9], [10], [11]. In addition, polymer semi permeable membranes are widely employed in exchangers in other industrial processes including refrigeration [12] and desalination applications[13]. Some of the properties of a membrane such as its thickness, porosity, thermal conductivity, and mass conductivity affect the efficiency of the heat and mass exchangers [14]. Mass conductivity, also known as water vapor permeability, has a main impact on the transport of water vapor within the membrane and thus on the overall performance of the membrane based exchangers [15]. It is the measure of the amount of water vapor that passes from one medium to another through a material of a given thickness and surface area and at a defined unit of time. The water vapor transmission is induced by the difference in vapor pressure between the two different media caused by the difference in temperature and concentration [16], [17]. If the membrane is not permeable or has a very low permeability, water vapor would be trapped within the material causing condensation to occur if its temperature reaches the saturation one. Thus the internal moisture increases which in turn blocks the mass transfer of the membrane exchanger. The water vapor transmission rate of porous materials highly depends on the physical properties of the membrane such as its material and the dimensions of its pores [18]. In order to be able to compare this magnitude in different membranes, it is important to be sure that these membranes are analyzed and tested to the same test method and procedure [19]. This property has often been determined by standard tests such as the ISO 2528 [20] and ASTM E96 [21]. Some of these methods are the sweating guarded hot plate test [22] and the desiccant inverted cup test [23]. Another well known approach is the upright cup method as described in ASTM E96 standard used to determine the water vapor transmission in porous materials of low to moderate permeability [24]. Our paper focuses on this test because it is the most commonly used among all.

2. ASTM E96 Upright Cup Method

In the upright cup test, two approaches can be done to measure the water vapor transmission, a dry cup and a wet cup method. These two tests have similar experimental setups but with different conditions. In the former the cup contains a solid desiccant material while in the latter the desiccant is replaced with liquid water [25]. The ASTM standard explains that the wet cup method should be used whenever a high relative humidity is expected at the vicinity of the tested material while whenever relative humidity levels are lower a dry cup test should be used [26]. In

the dry test the desiccant absorbs the water vapor which migrates from the air in the environmental chamber through the porous material and then into the cup. While in the wet cup method water molecules move from the water side to the air side crossing the membrane [27] as shown in figure 1.

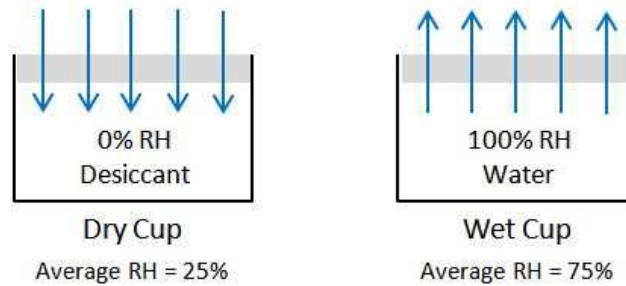


Figure 1: ASTM E96 upright cup test for measuring water vapor transmission

2.1 Procedure

The procedure for both tests is similar. A cup is filled either with a solid desiccant material or with distilled water leaving a small air space between them and the membrane. The sample of the porous material that needs to be tested is properly sealed to the edge of the cup to prevent side diffusion [28]. The initial weight of the cup is taken and then the cup is placed in an environmental chamber where the air temperature and relative humidity are continuously measured. The test cup is then weighed periodically to provide enough number of data points throughout the test. For the dry test measures weight is gained inside the cup due to the transfer of the water vapor from the chamber (high humidity) to the desiccant (low humidity). As for the wet test, it marks weight loss where the water vapor is transmitted from the cup (high humidity) to the atmosphere inside the chamber (low humidity).

2.2 Assumptions

The permeation values obtained from the tests of this standard depend on a set of conditions under which these tests are conducted. The following assumptions as mentioned in [29] and [30] are considered:

- An ideal sealing material should be used such that there is no weight gain or loss from or to the test chamber (evaporation, oxidation, hygroscopicity).
- A dish made of glass or any rigid, impermeable, corrosion-resistant material is preferred over lightweight metals like aluminum since oxidation might take place resulting in an increase of the cup weight.
- Three resistances are considered in the system, one caused by the air boundary layer R_a the other by the membrane R_m and the third by the air gap between the water surface and the membrane R_c as shown in figure 2.
- The total resistance of the system is equal to the sum of the individual resistances $R_{total} = R_a + R_m + R_c$. It can be calculated through Fick's law by equation (1).

$$R_{total} = \left(\frac{1}{\dot{m}}\right) D(\Delta c)A \quad (1)$$

where R is the resistance (exceptionally here it is expressed in meters), \dot{m} is the mass flux of water vapor, D is the diffusion coefficient of water vapor in air, Δc is the concentration difference and A is the area.

- The tested fabrics have low to moderate permeability which gives high resistance values.
- Air moving above the cups has a relatively high speed lowering its resistance. Thus the air side resistance R_a would not be calculated individually, it would be included with the resistance of the membrane R_m .
- The air cavity between the water surface and the membrane has a high resistance to vapor transfer that could be sometimes greater than that of the membrane itself.
- Mass transfer through this air gap is assumed to occur due to pure diffusion.

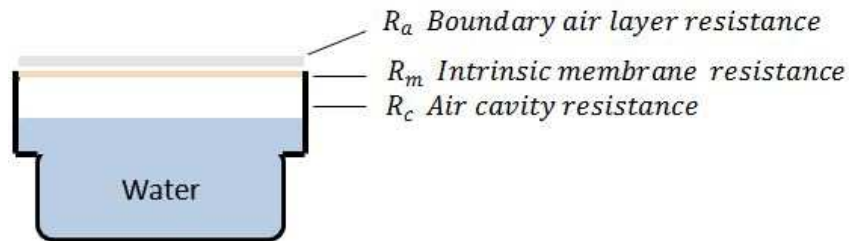


Figure 2: Three resistances to water vapor transfer in ASTM E96 standard

2.3 Discussion

The ASTM standard as indicated before is used to measure the water vapor transmission rate of materials with low to moderate permeability. Thus the resistance to mass transfer of such materials is high compared to that of air. Therefore as mentioned in the assumptions of the ASTM test, the value of the air side resistance is not calculated explicitly. Instead, it is estimated together with the resistance of the membrane being considerably smaller. This assumption is questionable when the tested fabrics have high permeability to water vapor. High permeability implies small resistance to heat and mass transfer and thus the resistance at the air side would not be negligible with respect to that of the fabric. In our experiments, we are interested in fabrics that allow a high water vapor transmission, to increase the efficiency of the exchangers, and thus the air resistance should be calculated separately. The ASTM E96 test doesn't provide data on how to calculate the resistances of highly permeable materials; hence this paper introduces a modified method to deduce the membrane mass conductivity by predicting the air resistance individually. This approach uses an identification methodology and will be explained later in this paper.

3. Modified Upright Cup Method

In order to find the mass transfer properties of some materials that could be employed as membranes, tests were conducted on three cups simultaneously containing hot water. One of the cups is remained uncovered and it stands as a control cup whose results are used later to deduce

the mass transfer coefficient of air. The other two cups are covered by two different samples of membranes with their edges properly sealed. A tiny air gap is kept between the water and the membrane which causes a water vapor mass transfer resistance. Yet, this gap cannot be neglected because it is necessary to reduce the risk of water touching the membrane. Figure 3 represents the schematic drawing of the modified method used in our experiment.

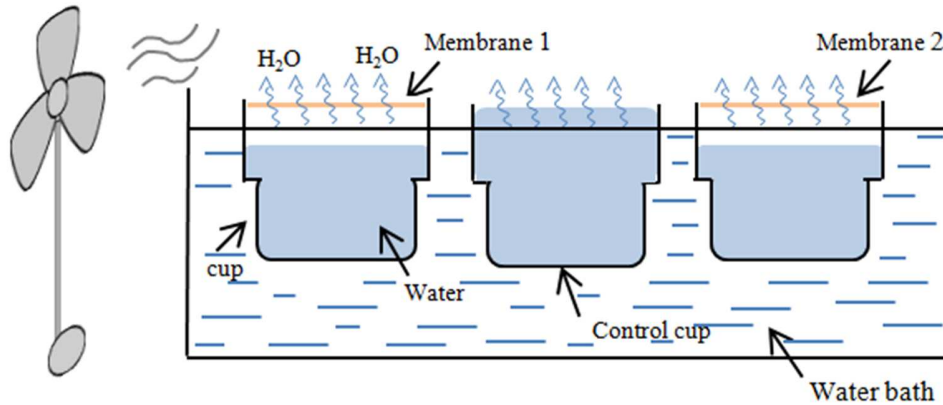


Figure 3: Schematic drawing of the modified cup method

The pans are maintained in a water bath of regulated temperature inside a room of ambient air at 25°C and 40% relative humidity. As described by the ASTM standard, a dry cup test is used when low relative humidity is expected at the vicinity of the tested material. Yet in our case water is used even though the ambient air relative humidity is not high enough. This is justified by the fact that in our application of the heat and mass membrane exchanger, the liquid (desiccant solution) is at a relatively high temperature which provokes a higher vapor pressure difference between it and the air outside and thus a higher heat and mass transfer. Therefore, for a true resemblance of our application, the water inside the cup is maintained at relatively high temperature.

A fan is turned on to force the air movement above the pans in order to decrease the air side mass transfer resistance. A temperature and water vapor concentration gradient difference exists between the water inside the pans and the air passing above them which creates a difference in the vapor pressure. Thus a vapor flow occurs from the water side through the permeable membranes towards the air side. The inlet temperature and the relative humidity of the air are continuously measured using a digital thermocouple and a hygrometer and the data is recorded. In addition, the temperature of the water inside the cups is repeatedly measured and periodic weighing of the test pans is made to determine the rate of water vapor transmission.

3.1 Experimental Conditions Assessment

The high temperature of water contributes to its high vapor pressure with a significant difference from that of the ambient air. Due to this difference the water vapor is going to be transferred through the membranes from the water side to the air side. The vapor is evaporated from the water at high temperature and comes in contact with the cool upper side of the membrane which has a temperature T_m . However, if the temperature of the water inside the cups was greatly higher

than that of air, a condensation process takes place by which the condensed water deposits on the membrane. When these droplets pile up on the lower surface of the membrane they fall back in the pan. In this case, the model representing the heat and mass transfer in the air gap between the liquid level and the membrane fails to be accurate and the results in term of membrane vapor permeability are not reliable. So in a way to be able to avoid the condensation problem, the temperature of the water should be kept just slightly greater than that of the air. Water vapor continues to be transmitted from the water to the air as long as the vapor pressure of the water is higher than that of air. The experiments are done with a water temperature between 30°C and 35°C and the mass of the water inside the pans is measured approximately every 10 to 15 minutes for around 6 hours.

3.2 Tested Membranes

Different fabrics that might have acceptable properties to act as membranes were chosen to examine their water vapor transmission rate and seven materials were tested. These materials include a membrane fabricated from electro-spun nanofiber and another from polypropylene. Other materials were permeable roof underlay material, Tyvek, and four non woven fabrics (NWF) used for pillow cases and sacs. These fabrics were selected to have different materials such that each has a different porosity and various thicknesses. We collected whatever low cost porous fabrics we came across that we thought they could be possible candidates. The main choice of these materials depended firstly on their prevention to liquid water permeation and secondly on their allowance to water vapor transfer. This makes them good candidates for being used as membranes in a heat and mass exchanger. The electro-spun nanofiber material was tested being a novel manufacturing technology. As for the polypropylene sheet this is because it is widely used in membrane exchangers and thus it would be interesting to compare its resistance with that the resistances of the chosen materials.

3.3 Experimental Data and Measurements

A total of 11 experiments were done, such that for every material the test is repeated 2 or 3 times. The conditions upon which the 11 experiments were performed are summarized in table 1 along with the results of the decrease in the water content in each cup.

Table 1: Input conditions of the different experiments along with the mass of water variation with time

Exp	Duration (h)	Membrane Type	Air average Temp (°C)	Air average RH (%)	Solution temp (°C)	Decrease in water content (g)
1	6.23	Control	24.6	44	30	14.11
		NWF-1				3.18
		NWF-2				2.86
2	7.4	Control	27.8	41.3	30	15.9
		Tyvek				2.34
		Electrospun nanofiber				2.85
3	6.6	Control	26.1	37.6	30	14.47

		Polypropylene				2.97
		Permeable roof underlay				1.18
4	6.55	Control	27.4	46.7	30	12.01
		Polypropylene				2.4
		NWF-1				2.84
5	6.34	Control	26.8	34.4	30	16.12
		NWF-3				2.78
		NWF-4				3.13
6	6.39	Control	26.3	35.7	30	17.01
		NWF-3				2.95
		Tyvek				2.24
7	7.35	Control	26.8	41.2	30	16.2
		NWF-2				3.22
		Permeable roof underlay				1.19
8	7.1	Control	27.9	36.1	34	19.81
		NWF-1				4.54
		NWF-4				4.08
9	7.18	Control	27	38.5	34	22.72
		Electrospun nanofiber				5.39
		Tyvek				3.43
10	7.06	Control	26.2	42.5	34	21.02
		NWF-1				4.89
		Electrospun nanofiber				4.68
11	6.19	Control	26.6	47.9	34	17.54
		Electrospun nanofiber				4.1
		Polypropylene				3.625

4. Deduction of Water Vapor Permeability

In the following section the methodology used to infer the water vapor permeability of the tested materials is discussed. At first the air resistance is deduced from the control cup as it is explained in the next paragraph.

4.1 Control Cup

4.1.1 Measurements

From the periodic experimental measurements, it can be shown that with time there is a decrease in the mass of water inside the cup. The mass variation of water inside the cups as a function of time can be plotted as curve (i) in figure 4a. This curve illustrates an example for the evolution of the water content in the control cup of experiment 1.

4.1.2 Numerical model

In the case of the control cup, due to the absence of a membrane, the only resistance is the air resistance. Thus the control pan is used in our experiment to deduce the real value of the mass transfer coefficient of the air which is dependent on the inlet air conditions (temperature, relative humidity and velocity). The mass transfer equation between the air and the water in the control pan is derived and expressed in equation (2).

$$h_{ma}A(Y - Y_w) = \frac{dm}{dt} \quad (2)$$

Where h_{ma} is the mass transfer coefficient of air in $\frac{kg}{m^2s}$, A is the exchange area between the air and the water in m^2 , Y is the absolute humidity in $\frac{kg}{kg(d.a)}$ and $\frac{dm}{dt}$ is the variation of the mass of water as a function of time in $\frac{kg}{s}$.

By solving equation (2) numerically using Modelica language in Dymola software, the curve of the variation of the mass of water as a function of time in experiment 1 is shown by curve (ii) in figure 4a.

➤ Deduction of the mass transfer coefficient h_{ma}

The optimization of the value of h_{ma} minimizes the error between curve (i) and curve (ii). Then when this error is minimal, this would give the value of the mass transfer coefficient of air h_{ma} as shown in figure 4b.

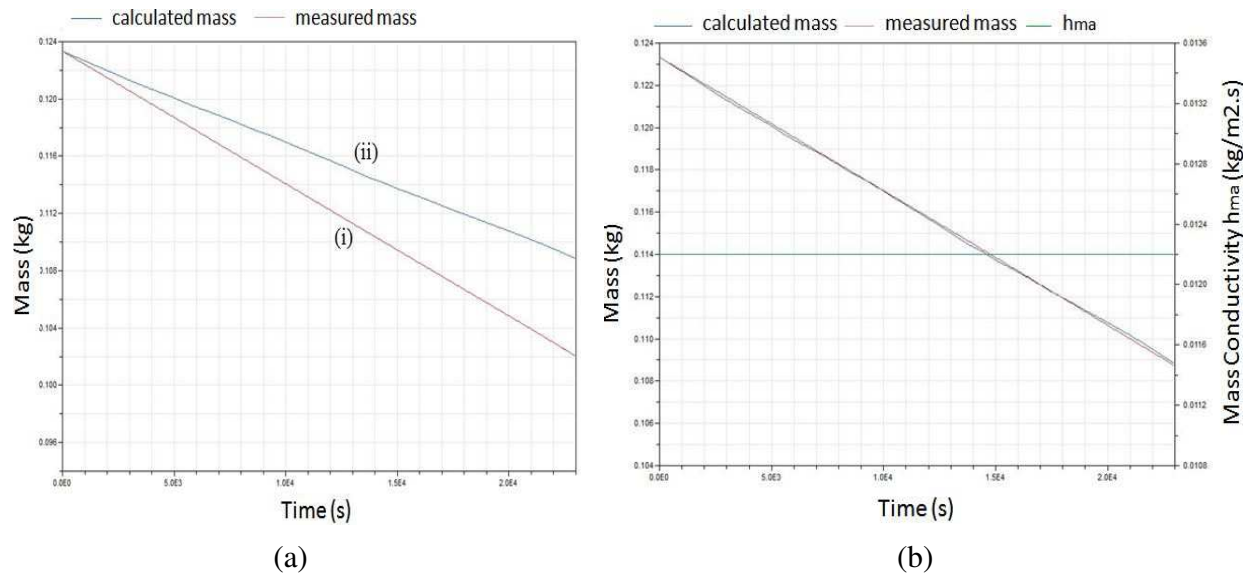


Figure 4: a) Variation of the measured mass (i) and calculated mass (ii) of water with respect to time in the control cup, b) mass conductivity of air determined by optimization

4.2 Cups Covered with Membranes

4.2.1 Measurements

From the periodic experimental measurements, we plot the curve of the mass variation of water as a function of time inside the cup covered with a membrane. This curve shows a decrease in the

water mass inside the cups which is less than that in the control cup. The curve (i) of the change in the water content of the cup covered with NWF-1 in experiment 1 is plotted in figure 5.

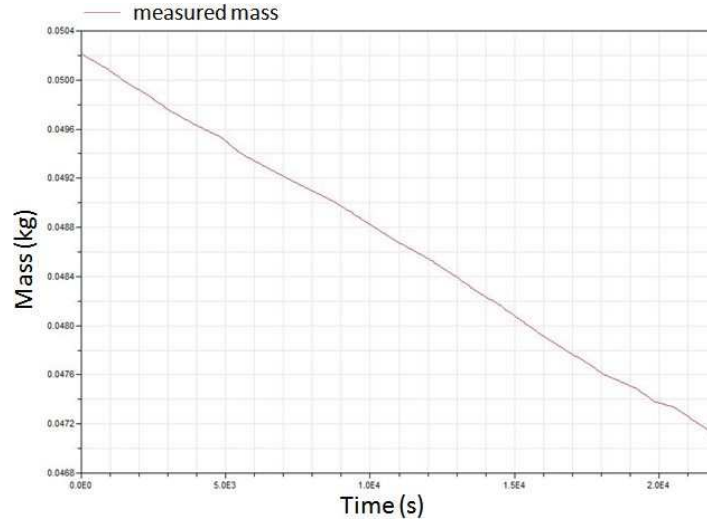


Figure 5: Variation of the measured mass (i) of water with respect to time in the cup covered with NWF-1 in experiment 1

4.2.2 Numerical model

The cups that are covered with membranes have a small air gap between the membranes and the water and this cavity has a resistance R_c . Figure 6 demonstrates the global resistance of the cup with membranes where the surface of the membrane can be considered at the interface of the two fluids.

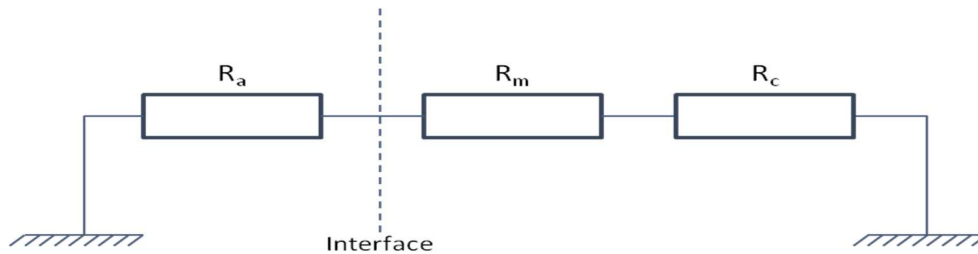


Figure 6: Diagram demonstrating the global resistance of the cups with membranes

With time the quantity of water inside the pans decreases thus this confined air space increases causing a decrease in its mass conductivity and hence an increase in its resistance. The overall resistance of the system can be represented by equation (3).

$$R_{total} = R_a + R_m + R_c = \frac{1}{h_{ma}} + \frac{\delta}{k_m} + \frac{1}{h_{mc}} \quad (3)$$

Where R is the resistance in $\frac{m^2s}{kg}$, δ is the thickness of the membrane in m , k_m is the mass conductivity of the membrane in $\frac{kg}{m.s}$ and h_{mc} is the mass transfer coefficient of the confined space in $\frac{kg}{m^2s}$.

➤ Heat and mass transfer in the confined space

In the confined space, the heat and mass transfer that takes place depends on the geometry and the orientation of the surfaces as well as on the thermo physical properties of the fluids involved. The characteristics of the heat transfer depend on whether the upper surface is the cold or the hot surface. If the cold surface is at the bottom and the hot surface is above, then no natural convection takes place since the lighter fluid will always be on top of the heavier fluid [31]; in that case, the mass transfer is purely diffusive. In our case, we have two horizontal surfaces where the lower is a hot surface (hot water) while the upper is a cold surface (membrane in contact with ambient air). The air adjacent to the hotter surface (which is lighter) rises and the air adjacent to the cooler surface (which is heavier) falls setting off a rotational motion that enhances the heat transfer by natural convection between the two surfaces. Therefore, the heat transfer coefficient of the air flowing naturally in the confined space should be calculated from correlations for natural convection between two isothermal surfaces.

➤ Data evaluation of the mass transfer coefficient h_{mc} inside the confined space

The heat transfer coefficient is related to Nusselt number by the formula $Nu = \frac{h_{Tc}L_c}{k}$ and the mass transfer coefficient is deduced by using the Lewis analogy $h_{mc} = \frac{h_{Tc}}{c Le^{\frac{2}{3}}}$. The Nusselt number is expressed as a function of Rayleigh number which in turn is expressed as a function of Grashof and Prandtl numbers. For a horizontal plate that represents an upper surface of a hot plate or a lower surface of a cold plate, the correlation for the Nusselt number is the following [31]:

$$Nu = 1 + 1.44 \left[1 - \frac{1708}{Ra} \right] + \left[\frac{Ra^{\frac{1}{4}}}{18} - 1 \right] \quad Ra < 10^8 \quad (4)$$

$$Nu = 1 + 1.44 \left[1 - \frac{1708}{Ra} \right] \quad Ra < 5832 \quad (5)$$

$$Nu = 1 \quad Ra < 1708 \quad (6)$$

$$\text{Where } Ra = Gr \cdot Pr = \frac{g\beta(T_h - T_c)L_c^3}{\nu^2} Pr \text{ and } \beta = \frac{2}{T_{hs} - T_{cs}}.$$

Where T_{hs} and T_{cs} are the temperatures of the hot and cold surfaces respectively. In our case, the temperature of the hot surface is considered to be equal to the temperature of the water. While the temperature of the cold surface, for more precision, it is considered to be equal to the temperature of the upper side of the membrane T_m which is in contact with the air (and not the temperature of air itself). In order to find T_m the energy or heat conservation equation of the system must be derived and it is expressed in (7).

$$h_{Tc}A(T_w - T_m) = h_{Ta}A(T_m - T_a) \quad (7)$$

Therefore, by calculating Rayleigh and Nusselt numbers, the convective heat and mass transfer coefficients in the confined space between the hot water and the membrane can be deduced.

➤ Deduction of k_m

The mass transfer equations of a cup covered with a membrane can be written as:

$$\frac{dm}{dt} = h_{mc}A(Y_{mw} - Y_w) \quad (8)$$

$$h_{ma}A(Y - Y_{ma}) = \frac{k_m}{\delta}A(Y_{ma} - Y_{mw}) \quad (9)$$

$$h_{mc}A(Y_{mw} - Y_w) = \frac{k_m}{\delta}A(Y_{ma} - Y_{mw}) \quad (10)$$

This system is used to solve for the unknowns of this equation that are Y_{ma} , Y_{mw} and k_m by substituting the value of the previously deduced mass conductivity of air h_{ma} and cavity h_{mc} in equations (8), (9), (10). Knowing the thickness of the membrane allows deducing the value of the mass conductivity of each membrane k_m .

Similar to the methodology used for the uncovered cup, we plot the curve (ii) of the calculated mass variation which is deduced from the system of equation as shown in figure 7a. Minimizing the error between these two curves allows us to find the mass conductivity of the membrane k_m as illustrated in figure 7b.

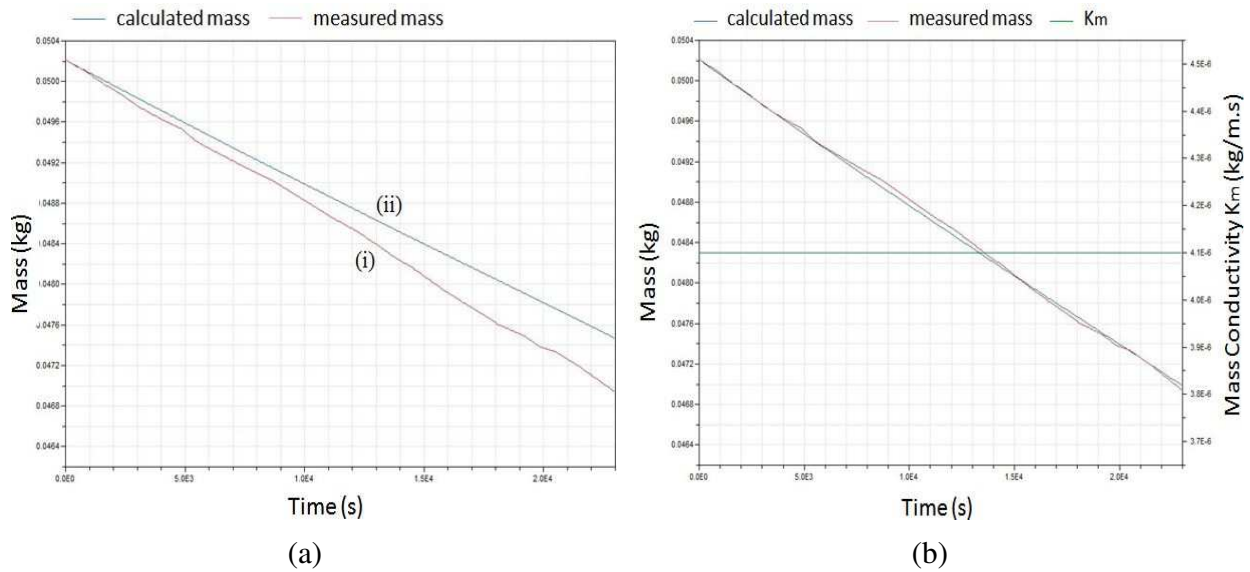


Figure 7: a) Variation of the measured mass (i) and calculated mass (ii) of water with respect to time in a covered up, b) mass conductivity of membrane determined by optimization

4.2.3 Results

Repeating the experiments several times, each time comparing two different membranes, enables us to classify the membranes according to their ability to transport water vapor. Each membrane is tested for between 2 and 3 times and for each test k_m is deduced by the same identification method. It is necessary to mention that in some of the performed tests, the result value of the

conductivity was largely far from the other deduced values for the same membranes. This is probably due to some measurement mistakes caused by accidental water spill. For this reason such results were discarded. The acceptable repeatable values (of all the performed tests) of the mass conductivity of each membrane are plotted in the graph of figure 8 from the highest to the lowest mass conductivity.

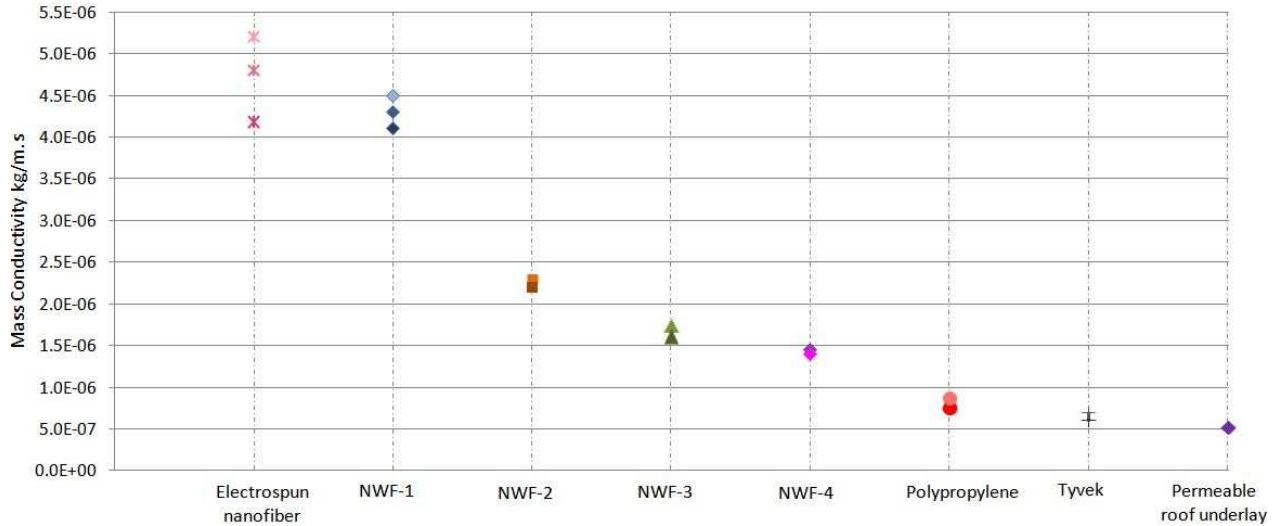


Figure 8: Mass conductivity results for all membranes from the 11 experiments

The average value of the mass conductivity of each membrane is then summarized in table 2. In this table also we can see the values of the resistance to heat and mass transfer which can be calculated by equation (11). The membranes are classified from the least to the most resistant to heat and mass transfer.

$$R_m = \frac{\delta}{k_m} \quad (11)$$

Table 2: The thickness, the average mass conductivity and the mass transfer resistance of all membranes

Membrane Type	Thickness (m)	Mass Conductivity k_m (kg/m.s)	Resistance R_m ($m^2.s/kg$)	Air resistance ($m^2.s/kg$)
Non-woven fabric-1	1.57E-04	4.30E-06	44	85
Electrospun nanofiber	2.56E-04	4.49E-06	68	85
Non-woven fabric-4	9.60E-05	1.43E-06	81	85
Non-woven fabric-2	1.67E-04	2.25E-06	89	83
Non-woven fabric-3	1.58E-04	1.68E-06	113	81
Polypropylene	8.00E-05	8.10E-07	119	88
Tyvek	1.50E-04	6.40E-07	281	80
Permeable roof underlay	4.05E-04	5.30E-07	917	86

This table shows that for membranes with low permeability (high resistance to mass transfer) the share of the air side resistance is relatively low with respect to the resistance of the membrane.

When the resistance of the material decreases the percentage share of the air side resistance increases. For highly permeable materials the share of the air side resistance is greater or approximately equal to that of the material which justifies the aim of our novel methodology. If the ASTM standard upright cup method was used to test these materials with high permeability the values of the mass conductivity of the membranes would be biased due to the relatively high values of the air resistance.

5. Uncertainty Analysis

In order to assess the method's accuracy for determining the membrane mass conductivity, an uncertainty analysis is performed because measurements are never made under perfect conditions, they are always subjected to certain errors and uncertainties [32]. Measurement uncertainty is a quantitative indication of the quality of the measurement results and of the confidence range concerning these results. The quality of measuring represents the accuracy of the results where it defines an interval by which the measured value lies around the true value. These measurements include the air temperature and relative humidity, the water temperature and mass as well as the thickness of the membrane and the diameter of the pan. Many conditions can affect the results of the readings of the measurements. Sometimes the measuring process itself is hard to make like in the case of the mass measurement of the water where the variation is very slow with respect to time. In other cases the measurement instruments can suffer from errors including bias or built in calibration uncertainty that influence the uncertainties of the measurements we take. These different uncertainties produced by each of these sources and other sources would be considered as inputs contributing to the overall uncertainty of the measurements done through the experiment. When different measuring instruments are used as in our experiment, in order to be able to evaluate the overall uncertainty of a certain value some main steps must be taken into consideration [33].

5.1 Methodology

➤ Definition of the measured and input sources

All the variables that directly or indirectly influence the determination of the measured quantities should be separately identified and they are known as the input sources.

➤ Modeling

Using the mass transfer equations (8), (9) and (10), the measured values are expressed as a function of the input sources. This phase helps visualize a cause-effect relation by knowing how the input sources affect the measured values.

➤ Estimation of the uncertainties of the input sources

There are two approaches to estimate uncertainties called 'type A' and 'type B' evaluation. 'Type A' evaluations are done using statistics when a set of several repeated readings is taken. In this case the average value as well as the standard deviation is deduced from these readings. While in 'type B' evaluations, the uncertainty is estimated from other information such as from calibration

certificates of instruments, from manuals and manufacturer's specifications or from estimates based on long-term experience.

➤ Estimation of PDF for the input sources

Estimate and select the most appropriate probability density function (PDF) that presents each of the input quantities. The spread of the set of values can take different forms such as a Gaussian distribution or a rectangular or uniform distribution. In our cases, we consider a typical normal Gaussian distribution where the values are more likely to fall near the mean rather than further away, i.e. 68% of the data falls within one standard deviation of the mean, 95% of the data falls within two standard deviations of the mean and 99.7% of the data falls within three standard deviations of the mean.

➤ Selection of the best approach for simulation

After all the input PDFs have been defined, one has to choose the best tool or approach to be able to successfully handle the different measurement uncertainties and to provide a reliable result of the output. One of the most reliable approaches used to estimate the measurement uncertainties is the Monte Carlo method which is adopted in our study for the following reasons [34]:

- It involves the propagation of the distribution of the input sources of uncertainties by using a model to provide the distribution of the output result.
- This method is easy to run, is faster and less tedious than other methods also the results are less subject to distortion.
- It can be successfully applied to cases where complex equations are used or whenever three or more measured variables are required for the uncertainty calculations.
- It effectively handles the probability distribution for each measured value; it allows us to choose any distribution as well as different distributions for different variables.

The Monte Carlo method uses the model to provide output distribution from the propagation of the distributions of input sources of uncertainty as illustrated in figure 9. The input quantities are represented by x_1 , x_2 and x_3 where $g(x_1)$, $g(x_2)$ and $g(x_3)$ are their distribution functions. The measurand is displayed as y and $g(y)$ is its distribution function [33]. When propagating distributions, the whole information contained in the input distributions are transmitted to the output. In our case, the model is non linear leading to a non direct relation between the inputs and the output. In such situation, it is possible to run simulations using on the model Monte Carlo method to find the combined standard uncertainty from the different individual ones.

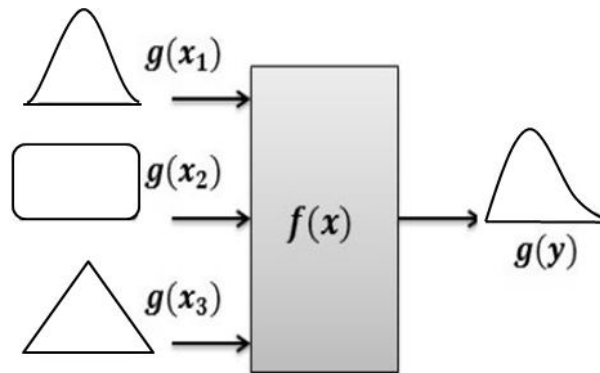


Figure 9: Illustrations of the methodologies of propagation of distributions [33].

5.2 Detailed Application of the Input Sources

A detailed application is presented for NWF-1 in experiment 8 where 17 measurements are taken with an average interval of 10 to 15 minutes between each. The Gaussian PDFs of the different inputs are derived by which every input source is represented as an array of 17 elements. Then a Monte Carlo approach is adopted where the total number of trials N is taken as 4000 which corresponds to the number of simulations done. Several input sources of uncertainty can be considered and they are expressed in the following:

➤ Air Temperature ($^{\circ}\text{C}$)

The data logger used to measure the input air temperature has a certified value for its temperature ranges, and its calibration certificate states an uncertainty of $\pm 0.3^{\circ}\text{C}$ at temperature 25°C . For every value of the temperature, a PDF is used where the mean is taken as the value of the measured temperature and the standard deviation is 0.3.

➤ Relative Humidity (%)

The data logger used to measure the air relative humidity has a certificate stating an uncertainty of 2% for a relative humidity measured at 25°C . Every value of the measured relative humidity stands as the mean of the PDF with a standard deviation equal to 2.

➤ Water Temperature ($^{\circ}\text{C}$)

To measure the temperature of water inside the pans, a thermocouple is used with a certificate stating an uncertainty of $\pm 0.3^{\circ}\text{C}$. So similar to the case of the air temperature, the mean of the PDF is the value of the measured temperature and the standard deviation is 0.3.

➤ Mass (kg)

The mass of the water inside the pans is obtained from weighing it periodically by a certified balance so several measured values are taken. The uncertainty associated with the mass using the data from the calibration certificate and the manufacturer's recommendations on uncertainty estimation is ± 0.01 g. So the uncertainty of each measured mass is represented by a separate PDF. The mean value of each PDF is taken as the measured mass value with a standard deviation of 10^{-5} kg.

➤ Thickness (m)

The thickness of the membrane is measured repeatedly for 16 times in a digital caliper with a capacity of 150 mm. This source of uncertainty is purely statistical and is classified as being of type A. The PDF that best represents this input source has a mean of 0.157 mm and a standard deviation of 5×10^{-6} m due to repeatability.

In addition, the caliper used for taking the measurements has a certificate stating an uncertainty of ± 0.03 mm. The uncertainty of the thickness due to the calibration of the caliper constitutes another source of uncertainty considered to be as type B involving the same input quantity (thickness). In this case the PDF used to represent this input uncertainty has a mean of zero and standard deviation of 3×10^{-5} m. The use of zero as the mean value is a mathematical artifice to take into account the variability due to this source of uncertainty without changing the value of the quantity used in the model. Then the combined PDF of the thickness of the membrane has a mean value of 1.57×10^{-4} m with a standard deviation of $\sqrt{(5 \times 10^{-6})^2 + (3 \times 10^{-5})^2} = 3.04 \times 10^{-5}$ m. Figure 10a represents the random change by N times of the thickness of the membrane around its mean.

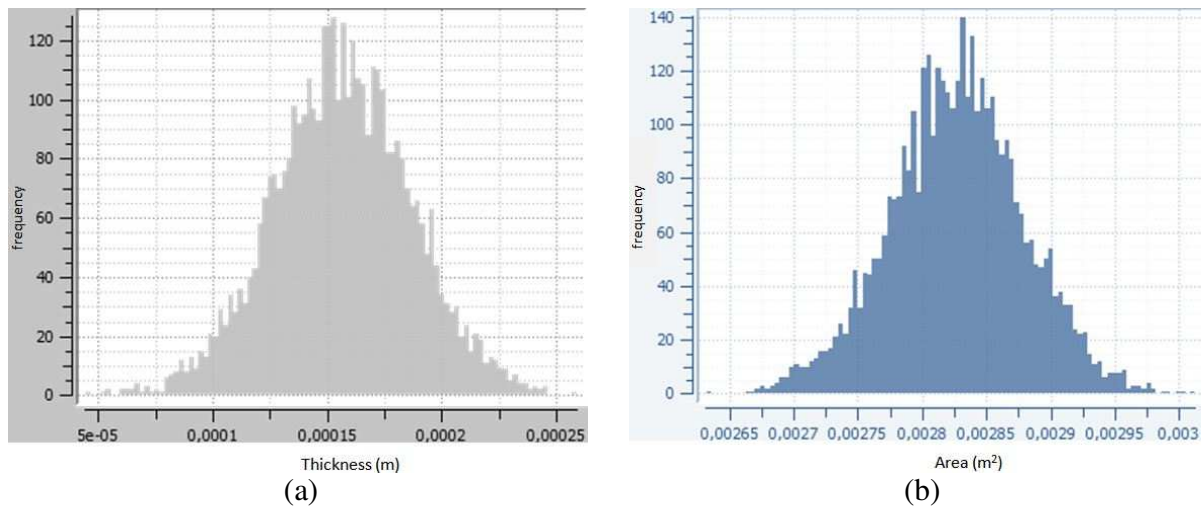


Figure 10: Histogram of a) thickness of the membrane b) exchange surface area

➤ Diameter (m)

The diameter of the pans was measured also 16 times with the same digital caliper. The mean value is 6 cm with a standard deviation of 5.5×10^{-2} cm. Then, the PDF of type A has a mean of 0.06 m and a standard deviation of 5.5×10^{-4} m. The type B uncertainty of the diameter of the pans is expressed with a mean value of zero and a standard deviation of 3×10^{-5} m. Thus the combined PDF of the diameter of the pan has a mean of 0.06 m and a standard deviation of 5.508×10^{-4} m.

➤ Area (m²)

The measurement of the diameter affects the value of the surface area of exchange between the water inside the pan and the air outside. The mean value of the diameter is 0.06 m so the mean value of the area is 0.0028274 m². The standard deviation of the diameter is 5.508×10^{-4} m so that

of the area is $5.19 \times 10^{-5} \text{ m}^2$. Figure 10b represents the change by N times of the exchange surface area of the membrane around its mean.

Table 3 summarizes the input sources of NWF-1 membrane with the type and PDF distribution of each parameter.

Table 3: A summary of the Gaussian PDF for all input uncertainties of NWF-1

Input source	Type	PDF	PDF parameters
Air Temperature (°C)	B	Gaussian	Mean: $T^c[i]$, std: 0.3°C
Relative Humidity (%)	B	Gaussian	Mean: $RH[i]$, std: 2%
Water Temperature (°C)	B	Gaussian	Mean: $T^c[i]$, std: 0.3°C
Water mass (kg)	B	Gaussian	Mean: $m[i]$, std: 10^{-5} kg
Thickness (m)			
Due to repeatability	A	Gaussian	Mean: $1.57 \times 10^{-4} \text{ m}$, std: $5 \times 10^{-6} \text{ m}$
Due to certificate	B	Gaussian	Mean: 0 m , std: $3 \times 10^{-5} \text{ m}$
Combined	A&B	Gaussian	Mean: $1.57 \times 10^{-4} \text{ m}$, std: $3.04 \times 10^{-5} \text{ m}$
Diameter (m)			
Due to repeatability	A	Gaussian	Mean 0.06 m , std: $5.5 \times 10^{-4} \text{ m}$
Due to certificate	B	Gaussian	Mean: 0 m , std: $:3 \times 10^{-5} \text{ m}$
Combined	A&B	Gaussian	Mean: 0.06 m , std: $5.508 \times 10^{-4} \text{ m}$
Area (m^2)			
Combined	A&B	Gaussian	Mean: $2.8274 \times 10^{-3} \text{ m}^2$, std: $5.19 \times 10^{-5} \text{ m}^2$

5.3 Results

By following the same procedure, the uncertainty study is done for every material considering only one experiment for each. The input uncertainty sources are deduced in each experiment and then the mass conductivity of each membrane is calculated by performing simulations. We control Dymola through Python and run the simulation for 4000 times while substituting the actual values of the air temperature and relative humidity, the water temperature, the measured mass, the thickness of each membrane and the exchange area by their previously determined Gaussian PDFs. The simulation for one experiment gives 4000 values of the mass conductivity of the membrane k_m . We determine $k_{m,mean}$ the mean for these values with its standard deviation std then the percentage uncertainty is calculated by the equation (12). Table 4 gives the values of the output uncertainties of the different membranes.

$$u = \frac{std}{k_{m,mean}} * 100 \quad (12)$$

Table 4: Percentage uncertainty for the tested membranes

Membrane Type	std (kg/m.s)	$k_{m,mean}$ (kg/m.s)	Uncertainty (%)
Non-woven fabric-1	7.84E-07	4.30E-06	17.43
Electrospun nanofiber	8.17E-07	4.49E-06	15.41
Non-woven fabric-4	3.93E-07	1.43E-06	26.23
Non-woven fabric-2	2.78E-07	2.25E-06	12.64
Non-woven fabric-3	3.29E-07	1.68E-06	21.98

Polypropylene	1.43E-07	8.10E-07	16.86
Tyvek	8.43E-08	6.40E-07	14.05
Permeable roof underlay	4.14E-08	5.30E-07	7.96

The values of the mass conductivities of the membranes with their standard deviations are shown on the graph of figure 11. They are plotted in decreasing order of mass conductivity. From this graph we can observe that even if the uncertainty on the mass conductivity is relatively high, yet the classification of the membranes by decreasing order of permeability would not change remarkably.

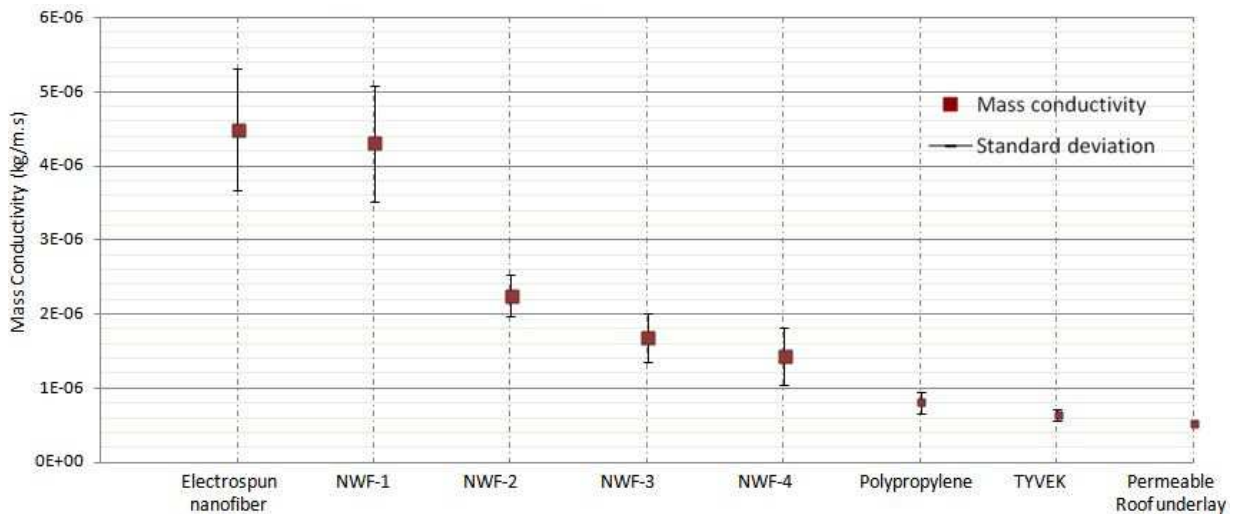


Figure 11: Mass conductivities of the different membranes with their error distribution

6. Conclusion

Water vapor permeability is the main property of membranes that influences its capacity of mass transfer. In this paper different possible low cost materials that are initially manufactured for considerations other than operating as membranes were identified. These materials were tested experimentally using a modified cup test and an identification methodology in order to find out their water vapor permeability. In this methodology we succeeded to deduce explicitly the value of the resistances at the air above the cups and of the air trapped between the water and the fabric. By substituting these values in the system of mass equations, the mass conductivities of the materials were determined. These values ranged from 5.3×10^{-7} to 4.49×10^{-6} kg/m.s. Thus measuring, analyzing and then interpreting the results for the different materials allow us to classify and compare the mass transfer capacity of each. Then an uncertainty analysis was performed to assess the accuracy of this approach and Monte Carlo method was used to evaluate the uncertainty propagation. The practical use of Monte Carlo simulations on the estimation of uncertainties has proved to be a fundamental tool in this area, being able to address complex measurement problems. The results showed that the uncertainty values varied from around 8% to 26%. These figures, although cannot be considered low enough, yet, it was seen that they didn't bring a change to the classification of the tested fabrics by order of the water vapor permeability. In further steps, the fabrics with a high mass conductivity (low resistance to heat and mass

transfer) and that possess the characteristics of being permeable to vapor, impermeable to liquid and capable to withstand water pressure can be employed as membranes in heat and mass exchangers. In addition, an analysis of the impact of the uncertainty of the mass conductivity on the total power of the heat and mass exchanger may be done. This would give an idea whether these large uncertainty values on k_m have a great effect on the numerical results of the performance of the exchanger or not.

Nomenclature

A	<i>area, m^2</i>
c	<i>concentration, g/m^3</i>
D	<i>diffusion coefficient of water vapor in air, m^2/s</i>
h_m	<i>mass transfer coefficient, $kg/m^2.s$</i>
h_T	<i>heat transfer coefficient, $W/m.K$</i>
k_m	<i>mass conductivity of the membrane, $kg/m.s$</i>
m	<i>mass, kg</i>
\dot{m}	<i>mass flux of water vapor, g/s</i>
N	<i>number of trials in Monte Carlo method</i>
NWF	<i>non woven fabric</i>
PDF	<i>probability density function</i>
R	<i>resistance to heat and mass transfer, m^2s/kg (unless indicated otherwise)</i>
std	<i>standard deviation</i>
T	<i>temperature, K</i>
T^c	<i>temperature, $^{\circ}C$</i>
t	<i>time, s</i>
u	<i>uncertainty, (%)</i>
Y	<i>humidity ratio in moist air: mass of water vapor per kg of dry air, kg/kg</i>
Y_w	<i>moist air equivalent humidity ratio in water, kg/kg</i>

Greek symbols

δ	<i>thickness, m</i>
----------	----------------------------------

Subscripts

a	<i>air</i>
c	<i>cavity</i>
cs	<i>cold surface</i>
hs	<i>hot surface</i>
m	<i>membrane</i>
ma	<i>membrane-air</i>

mw membrane-water
w water

Acknowledgment

The authors would like to acknowledge of the support of ERANETMED Project SOL-COOL-DRY, ID number: ERANETMED_ENERG-11-138 under ERA-MET Initiative “EURO-MEDITERRANEAN Cooperation through ERANET joint activities of FP7 INITIATIVE ERANETMED.

References

- [1] X. Li, Y. Zhou, S. Yu, G. Jia, H. Li, and W. Li, “Urban heat island impacts on building energy consumption: A review of approaches and findings,” *Energy*, vol. 174, pp. 407–419, May 2019, doi: 10.1016/j.energy.2019.02.183.
- [2] P. Liu, M. Justo Alonso, H. M. Mathisen, and C. Simonson, “Energy transfer and energy saving potentials of air-to-air membrane energy exchanger for ventilation in cold climates,” *Energy Build.*, vol. 135, pp. 95–108, Jan. 2017, doi: 10.1016/j.enbuild.2016.11.047.
- [3] J. Eom, L. Clarke, S. H. Kim, P. Kyle, and P. Patel, “China’s building energy demand: Long-term implications from a detailed assessment,” *Energy*, vol. 46, no. 1, pp. 405–419, Oct. 2012, doi: 10.1016/j.energy.2012.08.009.
- [4] X. Yin, X. Wang, S. Li, and W. Cai, “Energy-efficiency-oriented cascade control for vapor compression refrigeration cycle systems,” *Energy*, vol. 116, pp. 1006–1019, Dec. 2016, doi: 10.1016/j.energy.2016.10.059.
- [5] C. Zhang, X. Xue, Y. Zhao, X. Zhang, and T. Li, “An improved association rule mining-based method for revealing operational problems of building heating, ventilation and air conditioning (HVAC) systems,” *Appl. Energy*, vol. 253, p. 113492, Nov. 2019, doi: 10.1016/j.apenergy.2019.113492.
- [6] D. T. Bui, M. Kum Ja, J. M. Gordon, K. C. Ng, and K. J. Chua, “A thermodynamic perspective to study energy performance of vacuum-based membrane dehumidification,” *Energy*, vol. 132, pp. 106–115, Aug. 2017, doi: 10.1016/j.energy.2017.05.075.
- [7] L.-Z. Zhang, C.-H. Liang, and L.-X. Pei, “Conjugate heat and mass transfer in membrane-formed channels in all entry regions,” *Int. J. Heat Mass Transf.*, vol. 53, no. 5, pp. 815–824, Feb. 2010, doi: 10.1016/j.ijheatmasstransfer.2009.11.043.
- [8] S. Qiu *et al.*, “An energy exchange efficiency prediction approach based on multivariate polynomial regression for membrane-based air-to-air energy recovery ventilator core,” *Build. Environ.*, vol. 149, pp. 490–500, Feb. 2019, doi: 10.1016/j.buildenv.2018.12.052.
- [9] S. Chai, X. Sun, Y. Zhao, and Y. Dai, “Experimental investigation on a fresh air dehumidification system using heat pump with desiccant coated heat exchanger,” *Energy*, vol. 171, pp. 306–314, Mar. 2019, doi: 10.1016/j.energy.2019.01.023.
- [10] L.-Z. Zhang and N. Zhang, “A heat pump driven and hollow fiber membrane-based liquid desiccant air dehumidification system: Modeling and experimental validation,” *Energy*, vol. 65, pp. 441–451, Feb. 2014, doi: 10.1016/j.energy.2013.10.014.
- [11] A. H. Abdel-Salam, G. Ge, and C. J. Simonson, “Performance analysis of a membrane liquid desiccant air-conditioning system,” *Energy Build.*, vol. 62, pp. 559–569, Jul. 2013, doi: 10.1016/j.enbuild.2013.03.028.

- [12] F. Asfand and M. Bourouis, "A review of membrane contactors applied in absorption refrigeration systems," *Renew. Sustain. Energy Rev.*, vol. 45, pp. 173–191, May 2015, doi: 10.1016/j.rser.2015.01.054.
- [13] C. Feng *et al.*, "Production of drinking water from saline water by air-gap membrane distillation using polyvinylidene fluoride nanofiber membrane," *J. Membr. Sci.*, vol. 311, no. 1–2, pp. 1–6, Mar. 2008, doi: 10.1016/j.memsci.2007.12.026.
- [14] F. Asfand, Y. Stiriba, and M. Bourouis, "CFD simulation to investigate heat and mass transfer processes in a membrane-based absorber for water-LiBr absorption cooling systems," *Energy*, vol. 91, pp. 517–530, Nov. 2015, doi: 10.1016/j.energy.2015.08.018.
- [15] D. Bastien and M. Winther-Gaasvig, "Influence of driving rain and vapour diffusion on the hygrothermal performance of a hygroscopic and permeable building envelope," *Energy*, vol. 164, pp. 288–297, Dec. 2018, doi: 10.1016/j.energy.2018.07.195.
- [16] A. Gurubalan, M. P. Maiya, and S. Tiwari, "Performance characterization of membrane dehumidifier with desiccants in flat-plate arrangement," *Energy Build.*, vol. 156, pp. 151–162, Dec. 2017, doi: 10.1016/j.enbuild.2017.09.040.
- [17] C. Che and Y. Yin, "A statistical thermodynamic model for prediction of vapor pressure of mixed liquid desiccants near saturated solubility," *Energy*, vol. 175, pp. 798–809, May 2019, doi: 10.1016/j.energy.2019.03.115.
- [18] P. Mukhopadhyaya, M. K. Kumaran, and J. Lackey, "Use of the modified cup method to determine temperature dependency of water vapor transmission properties of building materials," *J. Test. Eval.*, vol. 33, no. 5, pp. 316–322, 2005.
- [19] W. Li and Y. Yao, "Study on the method for testing the water vapor diffusion resistance of membranes," *Polym. Test.*, vol. 69, pp. 80–90, Aug. 2018, doi: 10.1016/j.polymertesting.2018.04.030.
- [20] "ISO 2528 Sheet materials – Determination of water vapour transmission rate – Gravimetric (dish) method.," International Organization for Standardization, Geneva, 1995.
- [21] "ASTM E 96 Standard Test Methods for Water Vapor Transmission of Materials.," ASTM International, West Conshohocken, PA, 2013.
- [22] J. Huang, "Sweating guarded hot plate test method," *Polym. Test.*, vol. 25, no. 5, pp. 709–716, Aug. 2006, doi: 10.1016/j.polymertesting.2006.03.002.
- [23] J. Huang and X. Qian, "Comparison of Test Methods for Measuring Water Vapor Permeability of Fabrics," *Text. Res. J.*, vol. 78, no. 4, pp. 342–352, 2008, doi: 10.1177/0040517508090494.
- [24] R. H. Nosrati and U. Berardi, "Hygrothermal characteristics of aerogel-enhanced insulating materials under different humidity and temperature conditions," *Energy Build.*, vol. 158, pp. 698–711, Jan. 2018, doi: 10.1016/j.enbuild.2017.09.079.
- [25] B. Seng, C. Magniont, and S. Lorente, "Characterization of a precast hemp concrete block. Part II: Hygric properties," *J. Build. Eng.*, Sep. 2018, doi: 10.1016/j.job.2018.09.007.
- [26] B. Murphy, "Terms of Confusion Part 2 Permeability Test Methods," *Sherwin-Williams Waterblog*, Feb-2010. [Online]. Available: <https://sherwinblogs.com/2010/02/01/terms-of-confusion-part-2-permeability-test-methods/>. [Accessed: 02-Nov-2018].
- [27] Joseph W. Lstiburek, "It's All Relative. Magic and Mystery of the Water Molecule," *ASHRAE Journal*, 02-Oct-2017.
- [28] J. Richter and K. Staněk, "Measurements of Water Vapour Permeability – Tightness of Fibreglass Cups and Different Sealants and Comparison of μ -value of Gypsum Plaster Boards," *Procedia Eng.*, vol. 151, pp. 277–283, 2016, doi: 10.1016/j.proeng.2016.07.377.

- [29] Sloane Taliaferro, "Documentation and testing of nineteenth-century lime wash recipes in the united states," 2015.
- [30] A. P. S. Sawhney, L. B. Kimmel, G. F. Ruppenicker, and D. P. Thibodeaux, "A Unique Polyester Staple-Core / Cotton-Wrap Yarn Made on a Tandem Spinning System," Dec. 1993.
- [31] F. P. Incropera, "Natural Convection," in *Fundamentals of Heat and Mass Transfer*, 6th ed., Hoboken, NJ: John Wiley, 2007.
- [32] S. Bell, "Measurement Good Practice Guide No. 11 (Issue 2)," p. 41, Aug. 1999.
- [33] P. R. Guimaraes Couto, J. Carreteiro, and S. P. de Oliveir, "Monte Carlo Simulations Applied to Uncertainty in Measurement," in *Theory and Applications of Monte Carlo Simulations*, W. K. V. Chan, Ed. InTech, 2013.
- [34] I. Farrance, "Uncertainty in Measurement: A Review of Monte Carlo Simulation Using Microsoft Excel for the Calculation of Uncertainties Through Functional Relationships, Including Uncertainties in Empirically Derived Constants," *Clin. Biochem. Rev. Aust. Assoc. Clin. Biochem.*, vol. 35, p. 37, Feb. 2014.